



Short communication

Ether-functionalized ionic liquid electrolytes for lithium-air batteries



Hirofumi Nakamoto^{a,*}, Yushi Suzuki^a, Taishi Shiotsuki^a, Fuminori Mizuno^a,
Shougo Higashi^b, Kensuke Takechi^b, Takahiko Asaoka^b, Hidetaka Nishikoori^a, Hideki Iba^a

^a Battery Research Division, Toyota Motor Corporation, Higashifuji Technical Center, 1200 Mishuku, Susono, Shizuoka 410-1193, Japan

^b Advanced Battery Lab., Toyota Central R&D Labs., Inc., 41-1 Yokomichi, Nagakute, Aichi 480-1192, Japan

H I G H L I G H T S

- DEME–TFSA ionic liquid is functionalized with ether has high O₂ radical stability.
- The O₂ supply is the rate-limiting to generate LiO_x in ionic liquid's electrolytes.
- DEME–TFSA system has high LiO_x generation activity and lithium ion supply.
- We demonstrate the improved performance of the Li–O₂ battery using DEME–TFSA system.

A R T I C L E I N F O

Article history:

Received 27 December 2012

Received in revised form

24 May 2013

Accepted 27 May 2013

Available online 10 June 2013

Keywords:

Ionic liquid

Ether group

Oxygen diffusion

Lithium diffusion

Lithium-air battery

A B S T R A C T

Ionic liquids composed of *N,N*-diethyl-*N*-methyl-*N*-(2-methoxyethyl)ammonium (DEME), *N*-methyl-*N*-methoxyethylpiperidinium (PP1.1o2) cations functionalized with ethers, *N*-methyl-*N*-propylpiperidinium (PP13), and *N*-butyl-*N*-methylpyrrolidinium (P14) cations and the bis(trifluoromethanesulfonyl) amide (TFSA) anion are investigated for application as electrolytes in non-aqueous lithium–oxygen (Li–O₂) batteries. The PP13–TFSA, P14–TFSA and DEME–TFSA ionic liquids have high oxygen radical stability. A comparison of the lithium supply capacity measured using pulse-gradient spin-echo NMR for ⁷Li nuclei and the oxygen supply capacity measured using electrochemical methods indicates that the oxygen supply is the rate-limiting step for the generation of lithium–oxygen compounds (LiO_x) in these ionic liquids with supporting electrolytes. The DEME–TFSA system has the highest LiO_x generation activity among the ionic liquid systems examined. We demonstrate the improved performance (output power, discharge–charge capacity and coulombic efficiency) of a Li–O₂ battery using the DEME–TFSA system compared with that using the PP13–TFSA system. The improvements observed for the DEME–TFSA system are attributed to the high LiO_x generation properties and lithium ion supply.

© 2013 Elsevier B.V. All rights reserved.

1. Introduction

The realization of a low carbon society is required to address global climate change issues. This will require a decrease in the use of fossil fuels and the development of electric vehicles (EVs) to reduce or eliminate the production of carbon dioxide by gasoline-consuming vehicles. The lithium ion (Li-ion) secondary battery has high reliability and higher energy density than other secondary batteries, and is used in current EVs. However, the cruising distance of current EVs is only approximately 100 km for a full charge due to insufficient battery capacity. Therefore, alternative secondary batteries that surpass the capacity of current Li-ion batteries and also have reduced size are attracting attention.

There are high expectations for the lithium–oxygen (Li–O₂) battery due to its high energy density and low cost because the active material is O₂ in the air. Bruce and colleagues first reported a Li–O₂ battery that could be discharged and recharged for 50 cycles to demonstrate the possibility of a rechargeable Li–O₂ battery [1]. However, non-aqueous Li–O₂ batteries that employ carbonate-based solvents for the electrolyte have a large voltage gap between the discharge and charge reactions because the carbonate solvents are mainly decomposed by the superoxide radical anion (O₂ radical anion) and lithium peroxide (Li₂O₂) [2], the details of which have also been reported [3]. Therefore, the development of solvents that have chemical stability in the presence of O₂ radical species is one key strategy in the development of non-aqueous Li–O₂ batteries.

Recently, various organic solvents, such as ethers [4–8], amides [9], dimethyl sulfoxide and acetonitrile [7], have been investigated as candidate electrolytes that have higher stability against O₂

* Corresponding author. Tel.: +81 55 997 9589; fax: +81 55 997 7879.

E-mail addresses: hiro@nakamoto.tec.toyota.co.jp, hama111jp@yahoo.co.jp (H. Nakamoto).

radical species than the carbonate-based solvents. However, these solvents have not exhibited sufficient stability against oxygen radicals [8,9]. We have proposed the *N*-methyl-*N*-propylpiperidinium bis(trifluoromethanesulfonyl)amide (PP13–TFSA) ionic liquid as an electrolyte solvent that provides a smaller voltage gap than that of carbonate-based solvents. Li_2O_2 was confirmed as the main discharge product with this solvent because of the high stability of PP13–TFSA against O_2 radical anions and Li_2O_2 itself [10]. The volatility of the electrolyte solvent is also an important issue to consider in the development of an open-type Li– O_2 battery, and Kuboki et al. have reported the operation of a battery in air that employs ionic liquids [11]. While ionic liquids have these advantages of stability and a smaller voltage gap for application as Li– O_2 battery electrolytes, the high viscosity of the ionic liquids results in battery capacity and output power that are lower than those that employ organic solvents.

In this paper, we report the properties of four ionic liquids concluding two ether functionalized ones for application as electrolyte solvents of Li– O_2 batteries and demonstrate actual battery performance with two of the ionic liquid electrolytes.

2. Experimental section

2.1. Chemicals

N-Methyl-*N*-propylpiperidinium bis(trifluoromethanesulfonyl)amide (PP13–TFSA) and *N*-butyl-*N*-methylpyrrolidinium TFSA (P14–TFSA) were purchased from Kanto Chemical Co., Inc. *N,N*-Diethyl-*N*-methyl-*N*-(2-methoxyethyl)ammonium TFSA (DEME–TFSA), *N*-methyl-*N*-methoxyethylpiperidinium TFSA (PP1.1o2–TFSA), and Li–TFSA were purchased from Nisshinbo Holdings Inc., Merck Ltd., and Kojundo Chemical Laboratory Co., Inc., respectively. The chemical structures of these ionic liquids are shown in Fig. 1. Ultrahigh purity Ar (>99.99%) and O_2 (>99.9%) gases were obtained from Taiyo Nippon Sanso Co., Inc. All chemicals used were reagent grade and were dried at 120 °C in vacuum. The concentration of water in the ionic liquids was measured using a Karl Fischer titrator (Hiranuma Sangyo Co., Ltd., AQ-300) and was confirmed to be less than 20 ppm.

2.2. Characterization

Viscosity was measured at 25 °C using a viscometer (Sekonic Co., Ltd., VM-10A) in an Ar atmosphere with less than 1 ppm O_2 and less than 1 ppm H_2O . The temperature during the viscosity

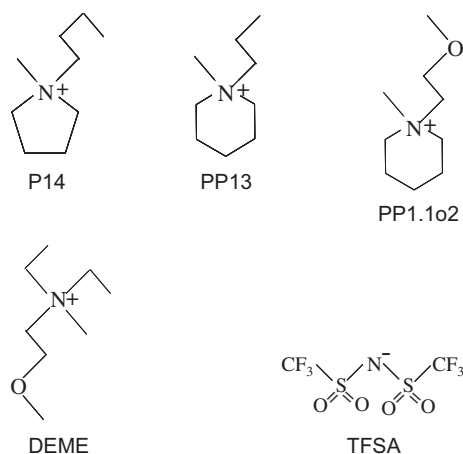


Fig. 1. Molecular structures of ionic liquids composed of the P14, PP13, PP1.1o2, and DEME cations and the TFSA anion.

measurements was controlled by using an incubator (Major Science, MC-01N).

Voltammetry and chronoamperometry measurements were performed with a three electrode cell system (BAS Co., Inc.) at 25 °C using a frequency analyzer (Solartron, SI 1255B) and a multichannel potentiostat/cell test system (Solartron SI 1470E). A glassy carbon disk (3.0 mm diameter) or a carbon fiber disk (5–11 μm diameter) was used as the working electrode, a nickel wire was used as the counter electrode, and a silver/silver cation (Ag/Ag^+) standard electrode was used as a reference electrode. The reference electrode consisted of a glass tube and a glass filter attached at the tip. An acetonitrile solution of 10 mM silver nitrate and 0.1 M tetrabutylammonium perchlorate was used as the electrolyte in the reference electrode, in which a silver wire was placed. The scan rate used for voltammetry was 10 mV s^{-1} . The temperature during the measurements was controlled with a constant-temperature chamber (Espec, SH-240).

The self-diffusion coefficient of lithium ions (D_{Li}) was measured at 25 °C using the pulsed-gradient spin-echo (PGSE) NMR method with a wide-bore 7.05 T superconducting magnet (SCM) equipped with a pulsed-field gradient (PFG) multiprobe (Jeol). The temperature was controlled at the NMR spectrometer (Agilent, INOVA300) console. The attenuation of the echo-signal E , was obtained by varying the duration time δ , of the PFG at a fixed amplitude, g . D_{Li} was determined according to the Stejskal equation [12]:

$$E = \exp\left[\gamma^2 g^2 \delta^2 D_{\text{Li}} (\Delta - \delta/3)\right], \quad (1)$$

where γ is the gyromagnetic ratio of the observing nuclei, and Δ is the interval period during the diffusion measurements. D_{Li} is independent of Δ in homogeneous samples, and as implied in Eq. (1), the single exponential echo attenuation indicates a free-diffusive mode. The measurement for ^7Li resonance was conducted by setting Δ at 50 ms, g at 13.75 T m^{-1} , and δ at 4 ms. The gradient parameters were selected to give 20 data points that spanned a signal attenuation of at least one order of magnitude.

2.3. Li–oxygen battery tests

The cathode of the Li– O_2 battery was prepared from a mixture of Ketjen Black (Ketjen Black International, ECP600JD) and polytetrafluoroethylene (PTFE; Daikin, battery grade) as a binder [2,10] in a 9:1 weight ratio. Disk-shaped (18 mm diameter, 80 μm thick) cathodes were formed and dried at 120 °C under vacuum. Li– O_2 cells were assembled in an Ar gas filled glove-box using the cathode disks, a 40 μm thick polyolefin separator, and the electrolyte containing each one of ionic liquids, and Li metal. The assembled Li– O_2 cells were evaluated with charge–discharge measurement apparatus (Nagano, BTS2004H). Current–voltage (I – V) tests were conducted using a current holding time of 15 min at current densities of 50 and 25 $\mu\text{A cm}^{-2}$, and cut-off voltages of 2.3 and 3.85 V, for discharge and charge, respectively. The cells were kept at the operating temperature (25 °C) for 3 h in an O_2 gas filled box prior to the electrochemical tests.

3. Results and discussion

3.1. O_2 radical stability of electrolytes

Fig. 2A presents the cyclic voltammograms of DEME–TFSA under both O_2 and Ar atmospheres. The potential sweep was started from +0.5 V to negative potential. The Fc^+/Fc potential in DEME–TFSA was 0.053 V vs. Ag/Ag^+ . The cyclic voltammogram measured for DEME–TFSA under an Ar atmosphere indicates electrochemical

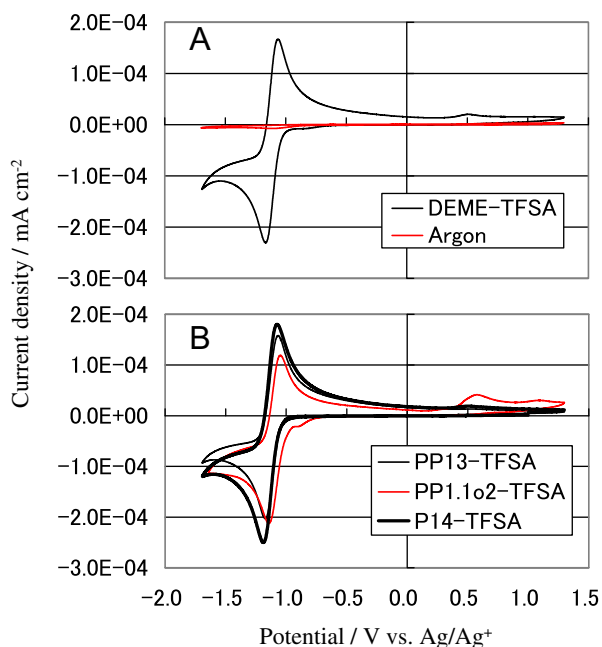


Fig. 2. Cyclic voltammograms for oxygen reduction in various ionic liquids at 25 °C: (A) DEME-TFSA with the Ar background, (B) P14-TFSA, PP1.1o2-TFSA and PP13-TFSA.

oxidation stability over +1.0 V vs. Ag/Ag⁺, which was similar to the other electrolytes examined. However, under an O₂ atmosphere, a reduction peak around −1.17 V and an oxidation peak around −1.05 V were observed, which are attributed to the generation and resolution of O₂ radical anions, respectively [13]. Fig. 2B shows the influence of oxygen on the other electrolytes (P14-TFSA, PP1.1o2-TFSA and PP13-TFSA). The Fc⁺/Fc potentials for P14-TFSA, PP1.1o2-TFSA and PP13-TFSA were 0.072, 0.063 and 0.070 V vs. Ag/Ag⁺, respectively. The oxidation current at +0.6 V is clearly observed under O₂ for PP1.1o2-TFSA, which is the lowest reversibility of O₂ reduction and oxidation capacities (56%) than the other electrolytes (DEME-TFSA: 72%, P14-TFSA: 76%, PP13-TFSA: 78%). Therefore the stability of PP1.1o2-TFSA toward O₂ radical anions may be insufficient for practical application.

3.2. O₂ gas supply capability

Fig. 3 shows chronoamperograms at −1.3 V measured for the DEME-TFSA solvent under Ar and O₂ atmospheres using a macro glassy-carbon disk electrode. The potential used in the measurements was determined to be below the rate-limiting O₂ reduction potential. The O₂ reduction current density (*i*_{O₂}) was obtained from the difference between the currents under O₂ and Ar atmospheres. The oxygen supply capacity (*C*_{O₂} × *D*_{O₂}^{0.5}) was calculated using the Cottrell equation [14]:

$$i_{O_2} = \frac{nFC_{O_2}\sqrt{D_{O_2}}}{\sqrt{\pi t}}, \quad (2)$$

where *C*_{O₂}, *D*_{O₂}, *n*, *t* and *F* are the O₂ solubility, the O₂ diffusion coefficient, the number of electrons, time, and Faraday's constant, respectively. The polarization time for the equation was determined from AC impedance measurements of the cell. The time to reach the rate-limiting current in the ionic liquids was longer than those in typical organic solvents due to the slower ion polarization. The steady-state current (*i*_{ss}) for a micro disk electrode with radius *r*, is given by Saito [15]:

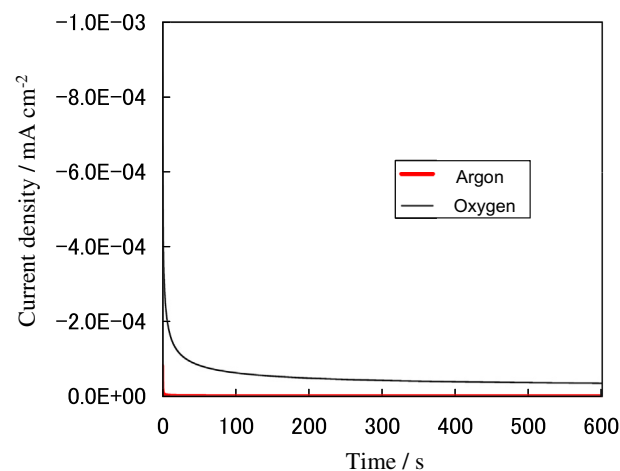


Fig. 3. Chronoamperograms for oxygen reduction and the Ar background in DEME-TFSA at 25 °C.

$$i_{ss} = 4nFC_{O_2}D_{O_2}r, \quad (3)$$

where *C*_{O₂} and *D*_{O₂} were calculated using Eqs. (2) and (3). The results for viscosity (*η*), *C*_{O₂} × *D*_{O₂}^{0.5} and *i*_{O₂} are given in Table 1. It has been reported that a Li–O₂ battery with a dimethyl sulfoxide (DMSO)-based electrolyte has a very large discharge capacity (ca. 3900 mAh g^{−1}-electrode) because of its low viscosity, *i.e.*, high O₂ and Li diffusion coefficients [19]. *C*_{O₂} for all the ionic liquid solvents is much lower than the solubility of lithium salt; therefore, the O₂ supply to the cathode will be insufficient. Accordingly, the O₂ supply capability of the electrolyte can be one of the rate-limiting factors of the Li–O₂ battery. Thus, high discharge capacities can be expected for Li–O₂ batteries with P14-TFSA and DEME-TFSA as electrolyte solvents with high O₂ diffusion coefficients. We have noted that even though *η* for DMSO is two orders of magnitude less than that of ionic liquids, *D*_{O₂} for these ionic liquids are in the same range as DMSO. This is most likely due to the size of the solvent molecule (see Fig. S11), although the details have yet to be clarified. Further understanding of the O₂ diffusion mechanism in the electrolyte is required for the development of high output Li–O₂ batteries.

3.3. Characteristics of the generation of lithium–oxygen compounds

Fig. 4 shows voltammograms for DEME-TFSA containing 0.35 mol kg^{−1} Li-TFSA. The Li-TFSA/DEME-TFSA electrolyte system under an Ar atmosphere has almost no reduction current, which is similar to that for DEME-TFSA without Li-TFSA (Fig. 2A). Under an O₂ atmosphere, oxidation peaks are detected at

Table 1
Physical properties of ionic liquids (including DMSO).

Solvent	<i>η</i> (cps)	<i>D</i> _{O₂} (cm ² s ^{−1})	<i>C</i> _{O₂} (mol cm ^{−3})	<i>C</i> _{O₂} √ <i>D</i> _{O₂} (mol cm ^{−1} s ^{−0.5})	<i>i</i> _{O₂} (mA cm ^{−2})
PP13-TFSA	259	3.0 × 10 ^{−6}	4.6 × 10 ^{−6}	8.0 × 10 ^{−9}	0.20
P14-TFSA	123	6.3 × 10 ^{−6}	3.9 × 10 ^{−6}	9.8 × 10 ^{−9}	0.25
PP1.1o2-TFSA	172	5.0 × 10 ^{−6}	3.6 × 10 ^{−6}	8.1 × 10 ^{−9}	0.21
DEME-TFSA	119	5.1 × 10 ^{−6}	4.4 × 10 ^{−6}	9.8 × 10 ^{−9}	0.23
DMSO	1.95 ^a	9.8 × 10 ^{−6b}	2.1 × 10 ^{−6c}		

^a Aminabhavi et al. [16].

^b Laoire et al. [17].

^c Sawyer et al. [18].

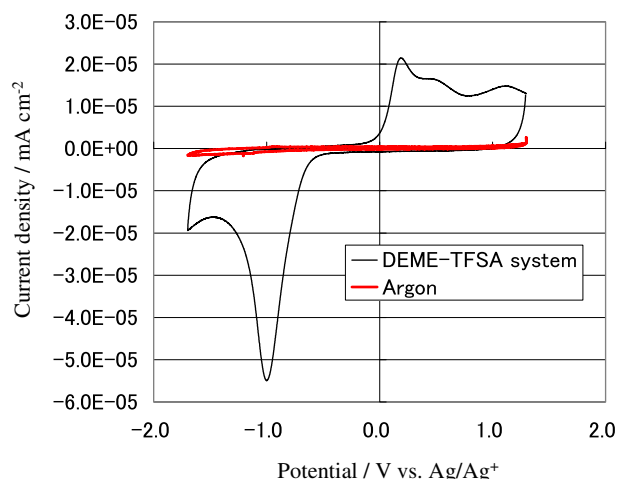


Fig. 4. Cyclic voltammograms for oxygen reduction and the Ar background in the DEME–TFSA system containing Li–TFSA at 25 °C.

Table 2
Li supply and voltammetric properties of various ionic liquid electrolytes containing Li–TFSA.

Solvent	D_{Li} ($\text{cm}^2 \text{s}^{-1}$)	C_{Li} (mol cm^{-3})	$C_{\text{Li}} \sqrt{D_{\text{Li}}}$ ($\text{mol cm}^{-1} \text{s}^{-0.5}$)	i_{LiO_x} (mA cm^{-2})
PP13–TFSA	2.1×10^{-8}	5.1×10^{-4}	74×10^{-9}	0.0143
P14–TFSA	4.1×10^{-8}	4.9×10^{-4}	99×10^{-9}	0.0369
PP1.1o2–TFSA	2.9×10^{-8}	5.0×10^{-4}	86×10^{-9}	0.0324
DEME–TFSA	4.5×10^{-8}	4.9×10^{-4}	104×10^{-9}	0.0388

around +0.33, +0.66 and +1.15 V, which are not resolution of oxygen radical anions. Furthermore, the reduction potential of the Li–TFSA/DEME–TFSA system (−1.00 V) is different from that of DEME–TFSA without a Li-salt (−1.16 V). The reduction current at around −1.0 V in the Li–TFSA/DEME–TFSA system is considered to indicate the generation of lithium–oxygen compounds (LiO_x).

The supply of lithium ions was estimated to confirm the rate-limiting reaction of LiO_x formation. The lithium ion supply capabilities ($C_{\text{Li}} \times D_{\text{Li}}^{0.5}$) of the ionic liquids measured by PGSE-NMR are shown in Table 2, where C_{Li} denotes the concentration of lithium ions. $C_{\text{Li}} \times D_{\text{Li}}^{0.5}$ in DEME–TFSA containing 0.35 mol kg^{-1} Li–TFSA at 25 °C was the same as that previously reported [20] and much higher than that of O_2 in DEME–TFSA (see Table 1). The current

for the generation of LiO_x in the Li–TFSA/DEME–TFSA system (i_{LiO_x} : $5.5 \times 10^{-5} \text{ A cm}^{-2}$) is much lower than the reduction current of O_2 gas in DEME–TFSA without the lithium salt (i_{O_2} : $2.3 \times 10^{-4} \text{ A cm}^{-2}$; see Table 1). In addition, $C_{\text{Li}} \times D_{\text{Li}}^{0.5}$ for all of the ionic liquids containing Li–TFSA are higher than $C_{\text{O}_2} \times D_{\text{O}_2}^{0.5}$ for the corresponding ionic liquids without lithium salts. Therefore, the rate-limiting reaction of LiO_x production in the ionic liquids is the O_2 gas supply capability. The DEME–TFSA system exhibited the highest LiO_x reactivity and lithium ion supply capability, as shown in Table 2. Therefore, it was concluded that the DEME–TFSA system is a promising candidate as an electrolyte for Li– O_2 batteries.

3.4. Performance of Li– O_2 battery

The I – V characteristics during the discharge process and discharge–charge curves for ionic liquid electrolytes containing 0.32 mol kg^{-1} Li–TFSA at 25 °C are shown in Fig. 5A and B, respectively. The current density and voltage of the DEME–TFSA system are higher than that of the PP13–TFSA system in Fig. 5A. Therefore, the power output of a Li– O_2 battery with the DEME–TFSA electrolyte system should be higher than that of the PP13–TFSA system.

The discharge and charge capacities of the DEME–TFSA system are three times as large as those of the PP13–TFSA system, as shown in Fig. 5B. In particular, the discharge capacity becomes over 3000 mAh g^{-1} -carbon without any catalyst in the cathode. The discharge plateau voltage of DEME–TFSA system is also higher than that of the PP13–TFSA system. The coulombic efficiencies for the first cycle, i.e., the reversibility of the charge capacity compared with the discharge capacity, for the DEME–TFSA and PP13–TFSA systems are approximately 66 and 24%, respectively. Discharge products were widely deposited on the cathode of the Li– O_2 cell with the PP13–TFSA electrolyte were relatively large (>100 nm) and larger than those deposited when using the DEME–TFSA electrolyte [21]. Li_2O_2 is an excellent electrical insulator; therefore, the smaller Li_2O_2 particles should be easily decomposed. Therefore, the DEME–TFSA system, which produces smaller Li_2O_2 particles as a discharge product, should reasonably improve the coulombic efficiency of a Li– O_2 battery. Such an improvement is the result of better O_2 supply capability to form smaller discharge products by the effect of uniform O_2 transport. The significant improvement of battery performance is attributed to the higher O_2 diffusion and lithium ion diffusion of the DEME–TFSA electrolyte due to its lower viscosity.

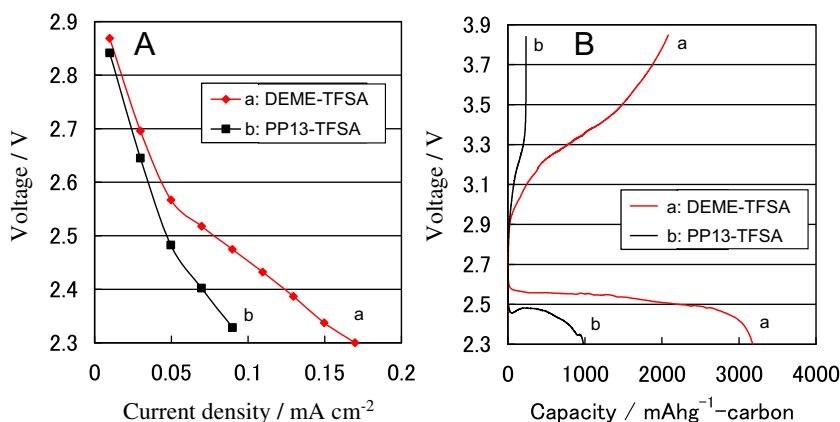


Fig. 5. Li– O_2 battery performance using ionic liquids (a: DEME–TFSA and b: PP13–TFSA) containing Li–TFSA at 25 °C: (A) discharge current density–voltage characteristics and (B) discharge–charge curves.

4. Conclusions

In this study, we have shown the advantages of ionic liquids as electrolytes for non-aqueous Li–O₂ batteries. PP13–TFSA, P14–TFSA, DEME–TFSA and PP1.1o2–TFSA have the required stability against electrochemical oxidation over 4 V vs. Li/Li⁺ for battery applications. PP13–TFSA, P14–TFSA and DEME–TFSA can also provide high O₂ redox reversibility, which is the one of the requirements for O₂ radical anion stability. Lithium ion supply, which was estimated using PGSE-NMR, is faster than O₂ gas supply in the electrolytes, which was measured using electrochemical methods. Therefore, O₂ supply in the DEME–TFSA system is the rate-limiting process for the formation of LiO_x as intermediate products of the proposed cathode reaction in a Li–O₂ battery. It can be concluded that the ether-functionalized ionic liquid, DEME–TFSA, has the highest LiO_x generation activity to realize superior O₂ supply capability for Li–O₂ battery applications. Improvement of the Li–O₂ battery performance (discharge–charge capacity, power output, and columbic efficiency) using a DEME–TFSA-based electrolyte is demonstrated and compared with that using a PP13–TFSA-based electrolyte. The ionic liquids also have properties such as non-volatility in addition to the proved properties above; therefore, these ionic liquids are considered to be promising candidate electrolytes for non-aqueous Li–O₂ batteries.

Appendix A. Supplementary data

Supplementary data related to this article can be found at <http://dx.doi.org/10.1016/j.jpowsour.2013.05.147>.

References

- [1] T. Ogasawara, A. Debart, M. Holzapfel, P. Novak, P.G. Bruce, *J. Am. Chem. Soc.* 128 (2006) 1390.
- [2] F. Mizuno, S. Nakanishi, Y. Kotani, S. Yokoishi, H. Iba, *Electrochemistry* 78 (2010) 403.
- [3] S.A. Freunberger, Y. Chen, Z. Peng, J.M. Griffin, L.J. Hardwick, F. Barde, P. Novak, P.G. Bruce, *J. Am. Chem. Soc.* 133 (2011) 8040.
- [4] J. Read, *J. Electrochem. Soc.* 153 (2006) A96.
- [5] W. Xu, J. Xiao, J. Zhang, D. Wang, J.G. Zhang, *J. Electrochem. Soc.* 156 (2009) A773.
- [6] W. Xu, J. Xiao, J. Zhang, D. Wang, J.G. Zhang, *J. Electrochem. Soc.* 157 (2010) A219.
- [7] C.O. Laoire, S. Mukerjee, K.M. Abraham, E.J. Plichta, M.A. Hendrickson, *J. Phys. Chem. C* 114 (2010) 9178.
- [8] S.A. Freunberger, Y. Chen, N.E. Drewett, L.J. Hardwick, F. Barde, P.G. Bruce, *Angew. Chem. Int. Ed.* 50 (2011) 8609.
- [9] Y. Chen, S.A. Freunberger, Z. Peng, F. Barde, P. Bruce, *J. Am. Chem. Soc.* 134 (2012) 7952.
- [10] F. Mizuno, S. Nakanishi, A. Shirasawa, K. Takechi, T. Shiga, H. Nishikoori, H. Iba, *Electrochemistry* 79 (2011) 876.
- [11] T. Kuboki, T. Okuyama, T. Ohsaki, N. Takami, *J. Power Sources* 146 (2005) 766.
- [12] E.O. Stejskal, *J. Phys. Chem.* 43 (1965) 3597.
- [13] Y. Katayama, H. Onodera, M. Yamagata, T. Miura, *J. Electrochem. Soc.* 151 (2004) A59.
- [14] A.J. Bard, L.R. Faulkner, *Electrochemical Methods, Fundamentals and Applications*, second ed., John Wiley & Sons, Inc., New York, 2001.
- [15] Y. Saito, *Rev. Polarogr.* 6 (1968) 177.
- [16] T.M. Aminabhavi, B. Gopalakrishna, *J. Chem. Eng. Data* 40 (1995) 856.
- [17] C.O. Laoire, S. Mukerjee, K.M. Abraham, E.J. Plichta, A. Hendrickson, *J. Phys. Chem. C* 114 (2010) 9178.
- [18] D.T. Sawyer, G. Chiericato, C.T. Angelis, E.J. Nanni, T. Tsuchiya, *J. Anal. Chem.* 54 (1982) 1720.
- [19] K. Takechi, S. Higashi, F. Mizuno, H. Nishikoori, H. Iba, T. Shiga, *ECS Electrochem. Lett.* 1 (2012) A27.
- [20] K. Hayamizu, S. Tsuzuki, S. Seki, Y. Ohno, H. Miyashiro, Y. Kobayashi, *J. Phys. Chem. B* 112 (2008) 1189.
- [21] F. Mizuno, K. Takechi, S. Higashi, T. Shiga, T. Shiotsuki, N. Takazawa, Y. Sakurabayashi, S. Okazaki, I. Nitta, T. Kodama, H. Nakamoto, H. Nishikoori, S. Nakanishi, Y. Kotani, H. Iba, *J. Power Sources* 228 (2013) 47.